Surface Modification by Plasma Etching and Plasma Patterning

Liming Dai,* Hans J. Griesser, and Albert W. H. Mau

CSIRO Division of Chemicals and Polymers, Private Bag 10, Rosebank MDC, Clayton, Victoria 3169, Australia

Received: February 13, 1997[⊗]

Using radio-frequency glow-discharge plasma techniques, we have prepared surface patterns of various chemical functionalities on a micrometer scale. While H_2O-plasma etching, discovered in this study, was used for generating surface patterns of oxygen-containing polar groups using a mask, surface patterning of various functionalities, including both polar and nonpolar groups, was achieved by plasma polymerization in a patterned fashion using appropriate monomer vapors and/or discharge conditions. Furthermore, we have developed a versatile method for obtaining patterned conducting polymers by first depositing a thin, patterned plasma polymer layer using a mask onto a metal-sputtered electrode and then performing electropolymerization of monomers such as pyrrole within the regions not covered by the patterned plasma polymer layer. The conducting polymer patterns thus prepared were shown to be electrically active.

Introduction

Radio-frequency glow-discharge plasma has been widely used for the surface modification of various materials. There exists a large body of literature on the modification of the surface properties of synthetic polymers by (nondepositing) plasma treatments or by the deposition of thin polymeric film coatings using plasma polymerization.[1] A large variety of chemical surface functionalities can be fabricated by plasma techniques, and plasma methods are particularly useful and versatile for polymers including perfluorocarbons and polyolefins that are amenable to only a limited range of conventional chemical reactions for surface modification. However, plasma modification of inorganic materials, such as cleaved mica sheets, seems to be much less discussed in the literature.[1,2] Owing to its unique properties, notably the ease with which transparent, *molecularly* smooth films can be obtained through a simple cleaving process, mica has been widely used as one of the most common substrates in the field of surface physical chemistry. For instance, mica sheets have been used as substrates for various measurements on atomic force microscopy (AFM),[3] scanning tunnelling microscopy (STM),[4] and surface force apparatus (SFA).[5] The general lack of other substrate materials with a molecularly smooth surface, but different surface chemistry, severely limits the use of these surface techniques for more advanced studies. On the other hand, surface functionalization of mica by *chemical* derivatization has proven to be difficult, since mica is very inert to most chemicals.[2] Recently, it has been demonstrated that this problem could be circumvented by firstly treating mica sheets with a water- or oxygen-plasma, which was reported to cause minimum disruption of the mica surface,[6] and then reacting the plasma-activated mica surface with saline, leading to the formation of a hydrophobic surface. Further derivatization could then introduce various other functional groups onto the plasma-modified mica surface.[6−8]

Although the water plasma treatment may not alter the surface topography of a substrate in most cases, we have recently found evidence for surface *etching* by the H_2O-plasma under certain conditions. This finding can be both an advantage and a hindrance. While the water-plasma etching may cause some undesirable surface roughness for the otherwise molecularly smooth mica sheet, it can also be used to create high-resolution surface patterns of hydrophilic regions on, for example, certain hydrophobic polymer films. More generally, we found that surface patterns of various specific functionalities on a micrometer scale could also be produced by plasma polymerization of appropriate monomers in a patterned fashion.

Pattern formation and recognition by the self-assembled-monolayer (SAM) technique has recently attracted a great deal of attention.[9−13] In particular, Rozsnyai and Wrighton[14] have used the SAM technique to pattern conducting polymers of polypyrrole, poly(3-methylthiophene) and polyaniline through selective electropolymerization of the corresponding monomers onto photochemically patterned disulfide SAMs on Au. Although the SAM technique provides an attractive approach for the pattern formation of conducting polymers on certain substrates, the very limited number of substrates, namely Si for silanes and Au for thiols or disulfides, which can be used for the formation of SAMs may preclude the general application of the SAM technique. In contrast, pattern formation by the plasma polymerization is a highly generic method, which ensures that the surface patterning methodology developed in this study can be readily transferred to many other systems. Furthermore, we have developed a versatile method for obtaining patterned conducting polymers by firstly depositing a thin patterned *nonconducting*[15] plasma polymer layer onto a metal-sputtered electrode and then performing electropolymerization of monomers, such as pyrrole and aniline. This leads to region-specific deposition of conducting polymers in regions free of the plasma polymer. The microlithographic formation of conducting patterns is a key prerequisite for various practical applications of conducting polymers, such as in integrated circuits, field-effect transistors, optical memory storage devices, and electroluminescent and electrochromic displays.[16] Our methods for patterning various chemical functionalities and/or functional polymers (e.g., conducting polymers) could find a wide range of practical applications in areas such as region-specific cell growth or protein fixation,[17,18] multichannel molecular recognition,[19] and lithographic fabrication of microelectronics.[16] In this paper, we present the detailed procedures used for generating high-resolution patterns of various surface functionalities through the H_2O-plasma etching and plasma/

* To whom correspondence should be addressed. E-mail: L.Dai@chem.csiro.au.

⊗ Abstract published in *Advance ACS Abstracts,* October 15, 1997.

S1089-5647(97)00562-2 CCC: $14.00

TABLE 1: Conditions for Plasma Etching and Polymerization

plasma	monomer pressure (Torr)	power (W)	frequency (kHz)	discharge duration (s)
H_2O	0.62	30	250	50
MeOH	0.99	30	375	120
n-hexane	0.55	35	150	90

electrochemical polymerization, together with some physicochemical characterization of the resulting surface patterns.

Experimental Section

Materials. Analytical grade methanol and *n*-hexane were purchased from Aldrich and used as monomers for plasma polymerization without further purification, whereas water was purified through an ultrapure water system (Milli-Q plus, Millipore). Prior to the plasma treatments, molecularly smooth mica sheets were obtained by freshly cleaving a muscovite mica sheet. Pyrrole and sodium perchlorate were purchased from Aldrich for the electrochemical work. Electron microscopy cover slips, cleaved mica sheets, perfluorinated ethylene−propylene copolymer (FEP), and polytetrafluoroethylene (PTFE) films coated with a gold or platinum layer were used as the substrates. Metal coating was performed using sputtering techniques.

Plasma Treatment and Electrochemical Polymerization. The equipment and the detailed procedures used for the (nonpatterned) plasma treatment have been previously described.[20] Briefly, the plasma etching was performed using a custom built reactor,[20] powered by a commercial radio-frequency generator operating between 150 and 375 kHz (ENI HPG-2). The plasma polymerization was carried out on the same plasma reactor, and pattern formation was achieved using a TEM grid as a mask. Table 1 lists discharge conditions for both the plasma etching and plasma polymerization. The steps for the plasma-patterning process are shown schematically in Figure 1.

For the pattern formation of conducting polymers, polypyrrole was region-specifically electrodeposited, from an aqueous (Milli-Q water) solution containing 0.1 M pyrrole and 0.1 M sodium perchlorate, onto a metal-sputtered surface precoated with a patterned plasma polymer layer. The electropolymerization was performed on an EG&G potentiostat/galvanostat (Model 273) using the potentiostatic mode by applying 0.75 V.[21] A one-component cell was used with the metal-sputtered substrates as the working electrode (ca. 1.5 cm^2) and a saturated calomel electrode (SCE) as reference. All potentials were referenced to the SCE.

Characterization. X-ray photoelectron spectroscopy (XPS) analyses were performed on a VG Escalab V spectrometer using non-monochromatic Mg Kα radiation at a power of 200 W.[20,22] XPS spectra were acquired at an emission angle of 75° relative to the surface normal. Atomic force micrographs (AFMs) were recorded on a Digital NanoScope III. Scanning electron micrographs (SEMs) were obtained using a Phillips XL-30 FEG SEM unit, while optical microscopic images were made on a Nikon Labophot-2 *reflection* light microscope. Advancing (ACA), sessile (SCA), and receding (RCA) air/water contact angles were measured on a modified Kernco G-II goniometer using the Milli-Q water as the test liquid.

Results and Discussion

Pattern Formation by Plasma Etching. *Water-Plasma Etching*. We have previously demonstrated that exposure of fluoropolymers, such as FEP and PTFE films, to H_2O-plasmas under vapor pressures in the range 0.3−0.5 Torr lowered the

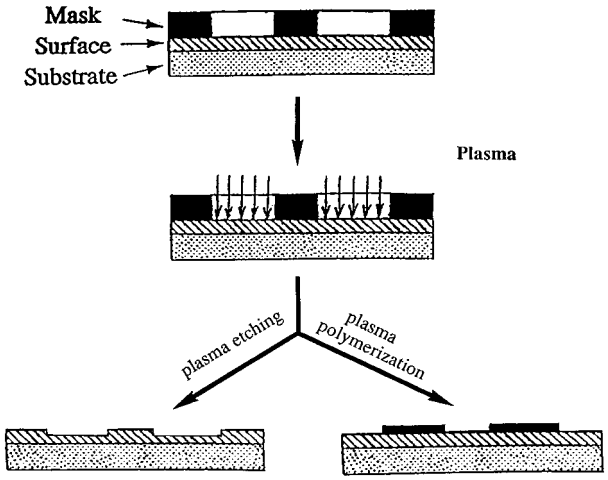

Figure 1. Schematic representation of pattern formation by the radio-frequency glow-discharge plasma techniques.

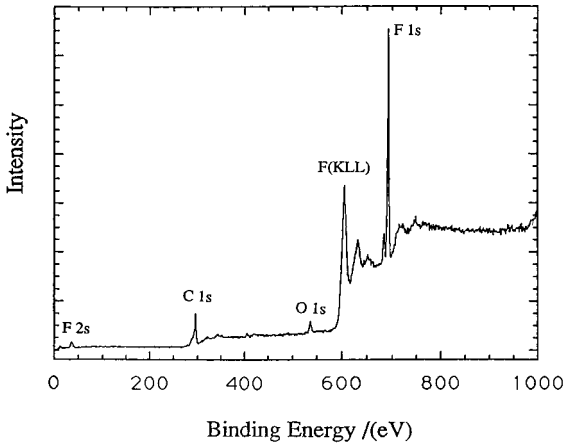

Figure 2. XPS survey spectrum of the H_2O-plasma-etched FEP surface.

air/water contact angles of the substrates. For instance, the SCA = 107°, ACA = 119°, and RCA = 98° for untreated FEP can be reduced to values of 80°, 90°, and 20°, respectively, by treating the FEP with the H_2O-plasma at 250 kHz, 30 W, and a monomer pressure of 0.34 Torr for 50 s. Recently, we have explored a wider range of discharge conditions and found a marked transition in the character of the water-plasma treatment by increasing the monomer vapor pressure. For example, SCA = 120°, ACA = 125°, and RCA = 7° were recorded for a FEP film treated by H_2O-plasma at 250 kHz, using a power of 30 W and a monomer pressure of 0.62 Torr for 50 s. While the low value of RCA indicates incorporation of oxygen-containing polar groups into the H_2O-plasma-treated surface, as confirmed by XPS analyses (Figure 2, O/C = 0.06), the very large extent of the contact angle hysteresis (i.e., the difference between ACA and RCA) may be attributed to the surface heterogeneity[23] caused by an inhomogeneous distribution of the fluorocarbon segments and the plasma-generated oxygen-containing polar groups. The unexpected contradiction between the increased SCA/ACA and incorporation of polar groups into the plasma surfaces may be rationalized by taking into account the effect of surface topography on contact angles. According to the Wenzel relation,[24,25] contact angles are expected to increase with increasing surface roughness if the initial value exceeds 90°. As we shall see later, topographical changes on the fluoropolymer surfaces were indeed observed for those polymer films treated with the "high"-pressure H_2O-plasma. The driving force for the H_2O-plasma-induced surface roughening arises, most probably, from the vapor pressure-enhanced $O_2^{\bullet+}$ concentration, which in turn leads to a high concentration of atomic oxygen

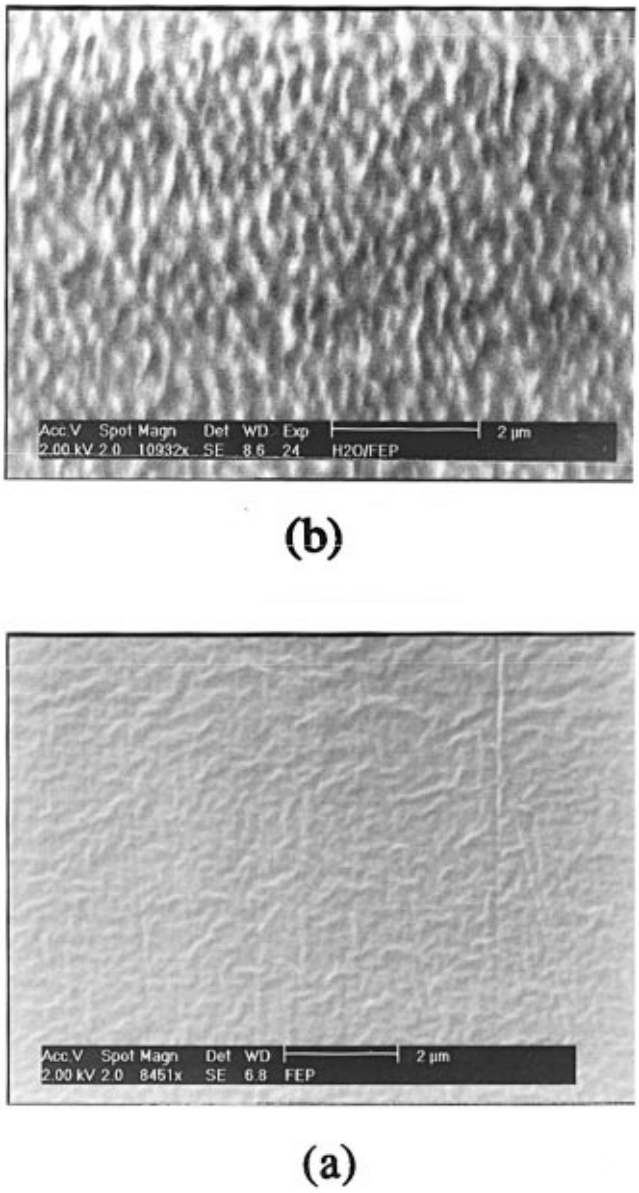

Figure 3. SEM micrographs of a FEP film (a) before and (b) after the H_2O-plasma etching.

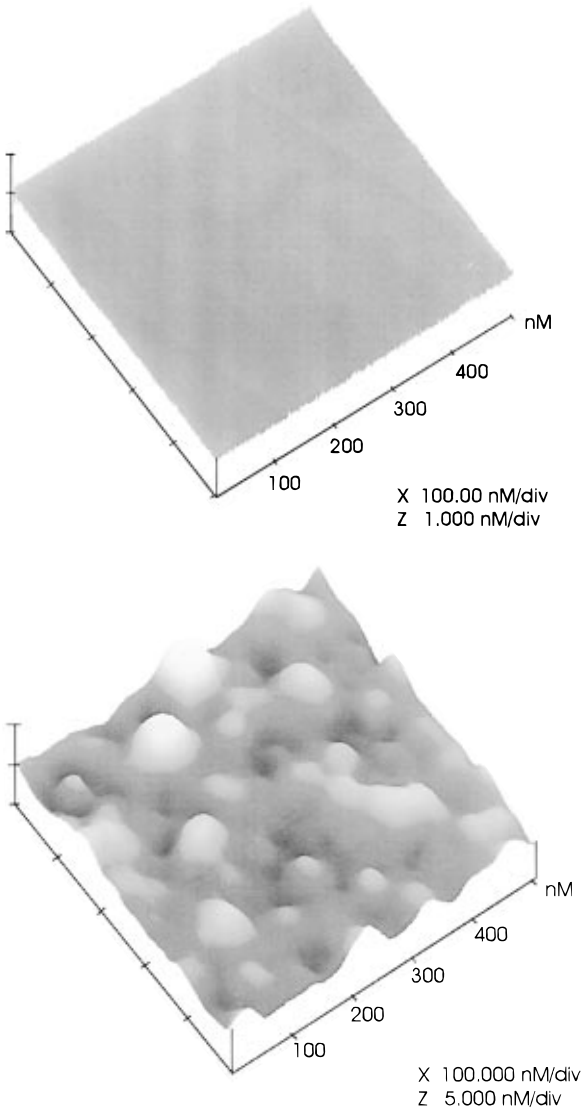

Figure 4. Typical AFM micrograph of (a, top) freshly cleaved mica surfaces and (b, bottom) after the H_2O-plasma etching.

in the "high"-pressure H_2O-plasma that could make a water-plasma very efficient for etching substrates.[26]

SEM studies show that H_2O-plasma treatment under the "high"-pressure conditions leads to a significant increase in the surface roughness for both FEP and PTFE, as exemplified by Figure 3. To investigate whether the H_2O-plasma under the "high"-pressure conditions could also etch other substrate materials and to test the suitability of the plasma-treated mica sheets for use as substrates for the highly surface-sensitive measurements (e.g., AFM, STM, SFA), we treated the freshly cleaved mica surfaces with the H_2O-plasma under conditions similar to those used for the etching of the fluoropolymers. Surface topography of the mica sheets before and after the plasma treatment was assessed by AFM. Figure 4a shows a typical AFM micrograph for the pristine mica surface. As expected, a molecularly smooth surface was observed. In contrast, the corresponding AFM image (Figure 4b) for the "high"-pressure H_2O-plasma-treated surface (250 KHz, 30 W, 0.68 Torr, and ca. 6 min) shows an average roughness as high as ca. 10 nm over a scanning area of ca. 500 × 500 nm. Caution should therefore be exercised when using the plasma-treated mica substrates with the molecularly sensitive analytical techniques such as AFM, STM, and SFA.[3−6]

H_2O-Plasma Patterning. As can be seen above, treatments by the H_2O-plasma under "high" monomer pressures enable the modification of the surface morphology with the simultaneous incorporation of oxygen-containing functional groups. The effects of these surface features on the attachment and/or growth of bioactive molecules (e.g., proteins, human cells) onto the modified surfaces should be of interest.[27] In this regard, we carried out the H_2O-plasma treatment in a patterned fashion for the purpose of generating patterned plasma surfaces of potential importance, for example, for region-specific cell growth or protein fixation.[17,18] The mask, a TEM grid, has grid bars of 7 μm and consists of hexagonal windows each with a size of ca. 50 μm. The resulting surface pattern was studied by SEM. As shown in Figure 5, patterned etching was obtained, with a close replication of the mask structure.

Pattern Formation by Plasma Polymerizations. Plasma polymerization enables the fabrication of thin polymeric coatings with a wide range of compositions, since almost all volatile organic vapors can be used as monomers in the process. For instance, the plasma polymerization of alcohol vapors, such as methanol or ethanol, produces hydrophilic thin films that are rich in hydroxyl groups.[28] Conversely, the use of *n*-hexane as a monomer vapor results in plasma polymer coatings of

Figure 5. Typical SEM micrograph of freshly cleaved mica sheets patterned by the H_2O-plasma etching with a TEM grid consisting of hexagonal windows as the mask (the line crossover the hexagonal structures is due to a crack in the mica sheet that occurred during the cleavage process in this particular case).

hydrophobic character.[20] We have used methanol and *n*-hexane as examples to fabricate patterned plasma polymer structures of hydrophilic and hydrophobic nature, respectively, as discussed in the following sections.

MeOH-Plasma Polymer Patterns. After sputter-coating a mica sheet with a thin gold film (the gold coating was required for the purpose of SEM imaging; see below), a methanol-plasma polymer layer was deposited. XPS analysis gave a survey spectrum (Figure 6a) that did not contain a signal from Au, indicating that the plasma polymer coating was at least 10 nm thick. The main peaks are assignable to C and O, with an O/C ratio of *ca*. 0.4. A third very weak signal, at ca. 399 eV, can be assigned to N; this element may be incorporated through post-treatment reaction with air on venting, as has been previously suggested.[29] The XPS C 1s spectrum, together with the curve fits using a Gaussian/Lorentzian product function[30] and a nonlinear Shirley background correction[31] is shown in Figure 6b. Numerical calculations based on the curve-fitted XPS C 1s spectrum show a high percentage of C−O groups for the MeOH-plasma polymer (Table 2). The significant incorporation of oxygen-containing polar groups in the MeOH-plasma polymer film is also manifested by the low values for the contact angles: SCA ≈ 40°, ACA ≈ 51°, and RCA ≈ 10°.

We will use the MeOH-plasma, as an example, to elucidate the procedures for patterning the −OH groups. In an initial experiment, MeOH vapor was directly plasma-polymerized onto freshly cleaved mica sheets or perfluoropolymer substrates in a patterned fashion using a TEM grid as the mask. Although the patterns thus obtained might be invisible to the naked eye, they were observable with SEM. However, it was found that charge built up rapidly upon exposure of the plasma surface to the SEM electron beam even at a relatively low accelerating voltage (*e.g.*, 1 kV). The surface charging not only prevented the detailed SEM examination of the plasma patterns but also caused permanent damage to the sample surface in some cases. This effect was shown to be caused by the insulating nature of the substrate surfaces, which cannot effectively dissipate either the charge or the heat generated by the electron beam. For subsequent experiments, therefore, the substrate surfaces (e.g., mica, FEP, PTFE) were coated by a gold or platinum film with a thickness of ca. 400 Å prior to the plasma treatments. In some cases, a thin chromium (ca. 30 Å thick) layer was precoated onto the mica surface to serve as an adhesion promoter between the mica and the gold or platinum layer. In addition

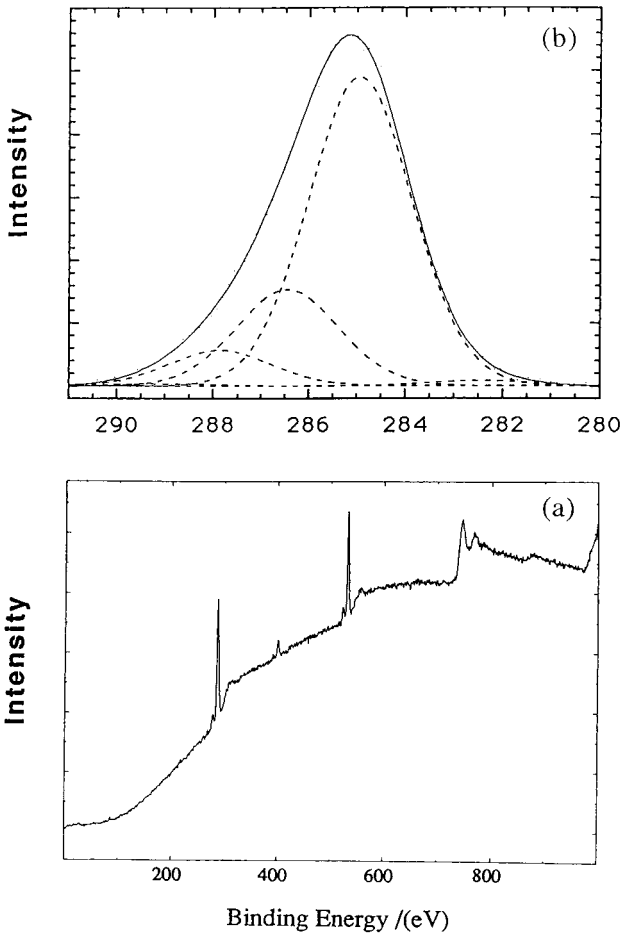

Figure 6. (a) XPS survey spectrum of a freshly prepared MeOH-plasma polymer onto a gold-coated mica sheet; (b) C 1s spectrum with a curve fit (see text).

TABLE 2: Composition of Carbon-Containing Surface Groups for the MeOH-Plasma Polymer Surface

C species	percentage contents
hydrocarbon (CH_x)	69.81
C−O	22.71
C═O	6.93
O−C═O	0.55

to the high electrical and thermal conductivities required for dissipating the surface charge and heat, the gold or platinum coating can also generate secondary electrons for pattern imaging.

Figure 7 shows a typical SEM micrograph of the patterns generated on a gold-coated mica surface by the patterned MeOH-plasma polymerization, with the dark areas representing MeOH-plasma polymer and bright regions being the uncovered gold surface. The plasma pattern thus formed is a close replication of the mask (TEM grid) structure with a resolution at the micrometer scale being clearly evident. The formation of the plasma-patterned SEM image is derived from the difference in scattering of secondary electrons, generated by the underlying gold, between the MeOH-plasma polymer and the uncovered gold surface. Generally speaking, the brightness of an insulating overlayer when it is exposed to a beam of electrons in the electron microscope is closely related to the yield of secondary electrons generated and emitted from the insulating surface.[11] Since scattering of the secondary electrons is expected to increase (and image brightness decrease) with increasing thickness of the insulating plasma polymer layer, the MeOH-plasma polymer becomes dark, while the uncovered gold regions are bright in Figure 7.

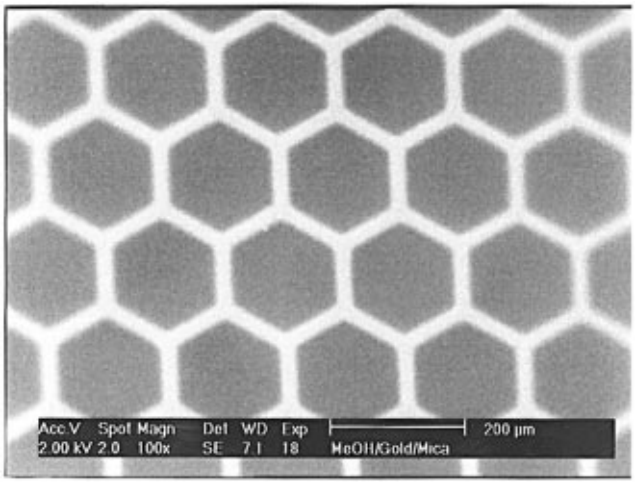

Figure 7. Typical SEM micrograph of the gold-coated mica sheets patterned by the MeOH-plasma polymer with a TEM grid consisting of hexagonal windows as the mask.

n-Hexane-Plasma Polymer Patterns. Having successfully demonstrated that both the H_2O-plasma etching and MeOH-plasma polymerization can be used for surface patterning polar groups (e.g., −OH), it is of interest to investigate whether nonpolar groups (e.g., alkyls) can also be patterned by the plasma technique. In so doing, we chose *n*-hexane as the plasma monomer to demonstrate the pattern formation of hydrocarbon surface groups. Owing to the generic nature associated with the plasma technique, other hydrocarbon molecules could also be used equally well as the plasma vapors for this purpose.

The deposition and spectroscopic characterization of *n*-hexane-plasma polymers have been previously reported.[20] These electrically insulating plasma polymer coatings change their surface characteristics on storage after deposition as a result of oxidative reactions[20] and surface restructuring.[32] Accordingly, freshly prepared *n*-hexane-plasma polymer coatings were used in this study. Figure 8a represents a typical XPS survey spectrum of the freshly prepared *n*-hexane-plasma polymer films. The films have contact angles of SCA ≈ 94°, ACA ≈ 105°, and RCA ≈ 66°. As expected, the dominant XPS signal in Figure 8a originated from carbon. A very weak oxygen signal was also observed, indicating a small extent of post-treatment oxidation of the plasma surface.[20,33] Atomic ratio calculations based on the XPS survey spectrum (Figure 8a) showed incorporation of oxygen into the plasma-treated surface to an O/C ratio of ca. 0.03. The chemical nature of the oxygen-containing groups was assessed by curve fitting of the XPS C 1s spectrum (Figure 8b). Numerical results are summarized in Table 3, which shows the relative contributions of C−O, C═O, and O−C═O groups. As can be seen in Table 3, the dominant contribution to the C 1s signal of the freshly prepared *n*-hexane-plasma polymer is from hydrocarbon groups, in good agreement with the results previously reported.[20]

The surface pattern generated by the patterned plasma polymerization of *n*-hexane is shown in Figure 9. In this figure the dark areas represent *n*-hexane-plasma polymer, and the bright regions are associated with the uncovered gold surface. It may be noticed, with care, that the contrast between the exposed and coated regions is greater for the MeOH-plasma polymer (Figure 7) than for the *n*-hexane-plasma polymer (Figure 9). Since both the MeOH- and *n*-hexane-plasma polymers have a similar film thickness (ca. 100 nm), the observed different in the image brightness is presumably related to the corresponding difference in surface compositions. This is because the SEM image brightness of a functionalized surface layer is inversely proportional to the electron density of the functional groups, leading to a darkened image for the functionalized surface with elements of high atomic number (for example, the SAM pattern of $C_{15}CH_2OH$ has a darker SEM image than that of $C_{15}CH_3$).[11]

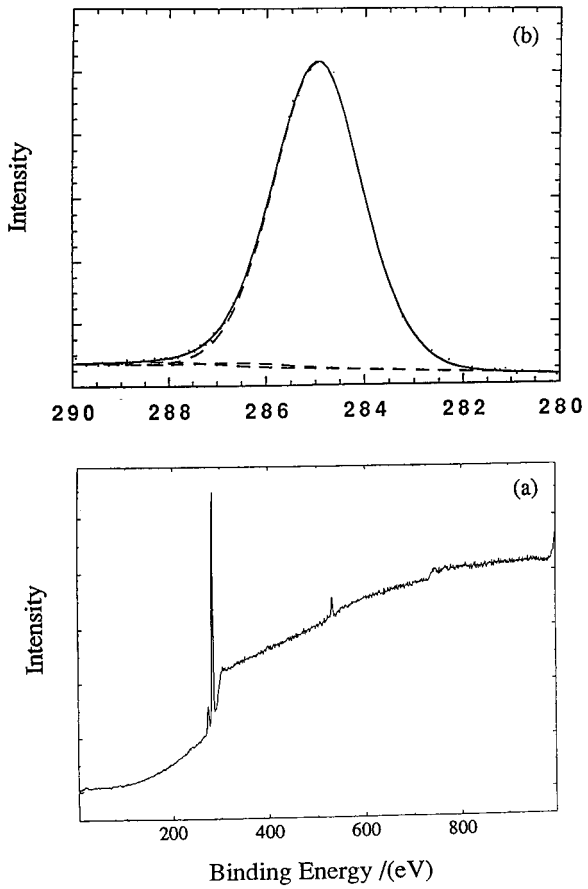

Figure 8. (a) XPS survey spectrum of a freshly prepared *n*-hexane-plasma polymer onto a gold-coated mica sheet; (b) C 1s spectrum with a curve fit.

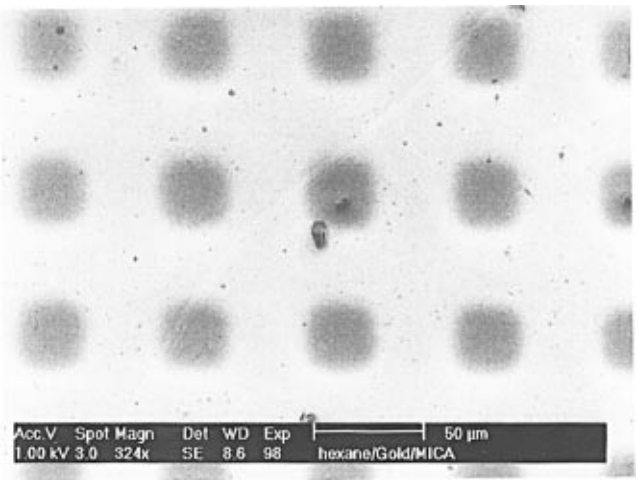

Figure 9. Typical SEM micrograph of the gold-coated mica sheets patterned by the *n*-hexane-plasma polymer with a TEM grid consisting of square windows as the mask.

TABLE 3: Composition of Carbon-Containing Surface Groups for the *n*-Hexane-Plasma Polymer Surface

C species	percentage contents
hydrocarbon (CH_x)	97.39
C−O	1.41
C═O	1.20
O−C═O	0.00

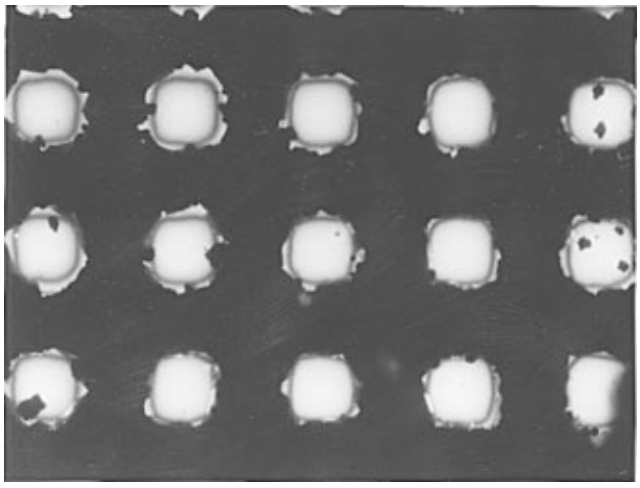

Figure 10. Optical microscopy image of a polypyrrole pattern electrochemically polymerized onto a platinum-coated mica surface prepatterned by the *n*-hexane-plasma polymer.

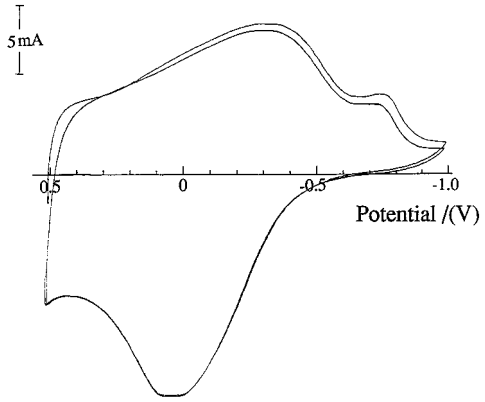

Figure 11. Typical cyclic voltammogram of the polypyrrole patterns on platinum at 100 mV s^{-1} in an aqueous solution containing 0.1 M sodium perchlorate.

Pattern Formation by Plasma/Electrochemical Polymerizations. As can be seen from the foregoing discussion, surface patterns of different chemical functionalities on a micrometer scale can be obtained using the patterned plasma polymerization method. We have also extended this technique to include conducting polymers using the plasma-patterned, metal-sputtered substrates as the electrode for electropolymerization. The governing principle for pattern formation with conducting polymers relies on the fact that the regions of the electrode surface covered by the plasma polymer are electrically insulating and hence inactive toward electropolymerization, whereas the uncovered areas can effectively initiate electropolymerization. Figure 10 represents a typical optical microscopic image of polypyrrole patterns electrochemically polymerized onto platinum-coated mica sheets prepatterned with the freshly prepared *n*-hexane-plasma polymer. It shows the same features as the plasma pattern of Figure 9, but with inverse intensities. The bright regions characteristic of the uncovered metal surface in Figure 9 become dark in Figure 10 due to the presence of a dark layer of the newly electropolymerized polypyrrole film. The bright regions in Figure 10 represent a more reflective surface associated with the *n*-hexane-plasma polymer.

The cyclic voltammetric response of a polypyrrole pattern thus prepared is shown in Figure 11, which is consistent with the published voltammograms.[14,21] Figure 11 clearly shows a reversible or quasi-reversible redox process with two reduction peaks for the polypyrrole film containing perchlorate. While the first reduction peak seen in Figure 11 can be attributed to the presence of a cationic species (polarons) in the polypyrrole film, the second reduction peak has been previously taken as evidence for the coexistence of a dicationic species (bipolarons).[21] As a control, the cyclic voltammetry measurement was carried out for a freshly prepared *n*-hexane-plasma polymer under the same conditions, which showed only small capacitive current with no peak attributable to the presence of any redox-active species. Therefore, the cyclic voltammogram shown in Figure 11 clearly indicates that the polypyrrole patterns prepared in this study are electrochemically active.

Conclusions

We have demonstrated that H_2O-plasma can cause surface etching of substrates under certain conditions. Using a mask, both H_2O-plasma etching and plasma polymerizations of appropriate monomers can produce surface patterns of various functional groups with micrometer resolution. This, coupled with electrochemical techniques, can be used to produce patterns of functional polymers, as exemplified by the conducting polypyrrole patterns generated through the plasma-patterning of *n*-hexane onto a metal sputtered electrode followed by the electropolymerization of pyrrole onto the plasma-polymer-free regions. These results have potential implication for the use of plasma (either the plasma treatment or plasma polymerization) patterning techniques for region-specific deposition of various chemical and/or biological functionalities, especially when they are used in conjunction with other surface derivatization methods.[34,35] Furthermore, our preliminary results show that surface patterns with distinctive regions of chosen chemical functionalities can be produced by *successively* carrying out the patterned plasma polymerization of different monomers, and the finding that different plasma polymers show different brightness in SEM micrographs may offer a relatively easy means for characterization of the surface distribution of functional groups in plasma polymer films by the SEM technique, as previously used for the SAM monolayers.[11,36]

Acknowledgment. We thank J.V. Ward and M.H. Greaves for assistance with the SEM work, L.O. Kolarik with the AFM measurements and T.R. Gengenbach with the XPS analyses.

References and Notes

(1) See, for example: Yasuda, H. *Plasma Polymerization*; Academic Press: Orlando, FL, 1985. d'Agostino, R. *Plasma Deposition, Treatment, and Etching of Polymers*; Academic Press: San Diego, 1990. Ratner, B. D. In *Comprehensive Polymer Science*; Aggarwal, S. L., Ed., Pergamon Press: New York, 1989; Vol. 7. Shen, M., Ed. *Plasma Chemistry of Polymers*; Marcel Dekker Inc.: New York, 1976. Hollahan, J. R., Bell, A. T., Eds. *Techniques and Applications of Plasma Chemistry*; John Wiley & Sons: New York, 1974.

(2) Okusa, H.; Kurihara, K.; Kunitake, T. *Langmuir* **1994**, *10*, 3577. Griesser, H. J. In *Storage Technology* (Proc. Am. Chem. Soc. Symp.); Mittal, K. L., Ed.; Plenum: New York, 1989. Bailey, S. W. In *Reviews in Mineralogy*; Vol. 13, Bailey, S. W. (Ed.), Mineralogical Society of America, BookCrafters, Inc.: Chelsea, 1984.

(3) Lea, A. S.; Pungor, A.; Hlady, V.; Andrade, J. D.; Herron, J. N.; Voss, E. W., Jr. *Langmuir* **1992**, *8*, 68. O'Shea, S. J.; Welland, M. E.; Rayment, T. *Langmuir* **1993**, *9*, 1826. Hamers, R. *J. Phys. Chem.* **1996**, *100*, 13103.

(4) Chiang, S. In *Scanning Tunneling Microscopy I*; Springer Series in Surface Sciences, Vol. 20; Guntherodt, H.-J., Wiesendanger, R., Eds.; Springer-Verlag: Berling, 1992. Edinger, K.; Golzhauser, A.; Demota, K.; Woll, Ch.; Grunze, M. *Langmuir* **1993**, *9*, 4.

(5) Dai, L.; Toprakcioglu, C. *Macromolecules* **1992**, *25*, 6000. Dai, L.; Toprakcioglu, C.; Hadziioannou, G. *Macromolecules* **1995**, *28*, 5512. Tripp, C. P.; Hair, M. L. *Langmuir* **1992**, *8*, 241.

(6) Parker, J. L.; Cho, D. L.; Claesson, P. M. *J. Phys. Chem.* **1989**, *93*, 6121.

(7) Wood, J.; Sharma, R. *Langmuir* **1994**, *10*, 2307.

(8) Parker, J. L.; Claesson, P. M.; Cho, D. L.; Ahlberg, A.; Tidblad, J.; Blomberg, E. *J. Colloid Interface Sci.* **1990**, *134*, 449.

(9) For a review, see: Whitesides, G. M.; Gorman, C. B. In *Handbook Surface Imaging Visualization*; Hubbard, A. T., Ed.; CRC Press: Boca Raton, FL, 1995. Ulman, A. *Chem. Rev.* **1996**, *96*, 1533. Whitesides, G. M.; Ferguson, G. S. *Chemtracts: Org. Chem.* **1988**, *1*, 171. Abbott, N. L.; Folkers, J. P.; Whitesides, G. M. *Science* **1992**, *257*, 1380.

(10) Kumar, A.; Whitesides, G. M. *Science* **1994**, *263*, 60.

(11) Lopez, G. P.; Biebuyck, H. A.; Whitesides, G. M. *Langmuir* **1993**, *9*, 1513.

(12) Frisbie, C. D.; Rozsnyai, L. F.; Noy, A.; Wrighton, M. S.; Lieber, C. M. *Science* **1994**, *265*, 2071.

(13) Schierbaum, K. D.; Weiss, T.; Thoden van Velzen, E. U.; Engbersen, J. F. J.; Reinhoudt, D. N.; Gopel, W. *Science* **1994**, *265*, 1413.

(14) Rozsnyai, L. F.; Wrighton, M. S. *J. Am. Chem. Soc.* **1994**, *116*, 5993; *Langmuir* **1995**, *11*, 3913.

(15) Radio-frequency glow-discharge plasma polymerization has been demonstrated to produce thin, cohesive, adhering polymer films,[1] which, in most cases, are electrically insulating although a few approaches to semiconducting plasma polymer films have been reported (see, for example: Golombok, M.; Gower, M. C.; Kirby, S. J.; Rumsby, P. T. *J. Appl. Phys.* **1987**, *61*, 122. Khor, E.; Munro, H. S.; Ward, R. J. *Polym. Mater. Sci. Eng.* **1990**, *62*, 677. Tanaka, K.; Yamabe, T.; Takeuchi, T.; Yoshizawa, K.; Nishio, S. *J. Appl. Phys.* **1991**, *70*, 5653. Tanaka, K.; Nishio, S.; Matsuura, Y.; Yamabe, T. *J. Appl. Phys.* **1993**, *73*, 5017. Nishio, S.; Takeuchi, T.; Matsuura, Y.; Yoshizawa, K.; Tanaka, K.; Yamabe, T. *Synth. Met.* **1992**, *46*, 243. Kojima, T.; Takaku, H.; Urata, Y.; Gotoh, K. *J. Appl. Polym. Sci.* **1993**, *48*, 1395. Tanaka, K.; Matsuura, Y.; Nishio, S.; Yamabe, T. *Synth. Met.* **1994**, *65*, 81. Gong, X.; Dai, L.; Mau, A. W. H.; Griesser, H. J. *J. Polym. Sci., Part A*, in press.

(16) Dai, L.; Griesser, H. J.; Hong, X.; Mau, A. W. H.; Spurling, T. H.; Yang, Y.; White, J. W. *Macromolecules* **1996**, *29*, 282, and references therein. Bowden, M. J., Turner, S. R., *Electronic and Photonic Applications of Polymers*; Advances in Chemistry Series 218; American Chemical Society: Washington, DC, 1988.

(17) d'Agostino, R., Ed. *Plasma Deposition, Treatment, and Etching of Polymers*; Academic Press: London, 1990.

(18) Voivodov, K.; Chan, W.-H.; Scouten, W. *Makromol. Chem., Macromol. Symp.* **1993**, *70/71*, 275. Ranieri, J. P.; Bellamkonda, R.; Jacob, J.; Vargo, T. G.; Gardella, J. A.; Aebischer, P. *J. Biomed. Mater. Res.* **1993**, *27*, 917. Pritchard, D. J.; Morgan, H.; Cooper, J. M. *Angew. Chem., Int. Ed. Engl.* **1995**, *34*, 91.

(19) Frisbie, C. D.; Rozsnyai, L. F., Noy, A., Wrighton, M. S.; Lieber, C. M. *Science* **1994**, *265*, 2071.

(20) Gengenbach, T. R.; Vasic, Z. R.; Chatelier, R. C.; Griesser, H. J. *J. Polym. Sci., Part A* **1994**, *32*, 1399.

(21) Kaplin, D. A.; Qutubuddin, S. *Polymer* **1995**, *36*, 1275.

(22) Dai, L.; St John, H. A. W.; Bi, J.; Zientek, P.; Chatelier, R. C.; Griesser, H. J. *Surf. Interf. Anal.*, in press.

(23) See, for example: Cassie, A. B. D.; Baxter, S. *Trans. Faraday Soc.* **1944**, *40*, 546. Cassie, A. B. D. *Discuss. Faraday Soc.* **1948**, *3*, 11. Marmur, A. *J. Colloid Interface Sci.* **1994**, *168*, 40. Morra, M.; Occhiello, E.; Garbassi, F. *Langmuir* **1989**, *5*, 872.

(24) Morra, M.; Occhiello, F.; Garbassi, F. *Adv. Colloid Interface Sci.* **1990**, *32*, 79.

(25) Morra, M.; Occhiello, E.; Garbassi, F. *Langmuir* **1989**, *5*, 872.

(26) Goldblatt, R. D.; Ferreiro, L. M.; Nunes, S. L.; Thomas, R. R.; Chou, N. J.; Buchwalter, L. P.; Heidenreich, J. E.; Chao, T.H. *J. Appl. Polym. Sci.* **1992**, *46*, 2189. Manos, D. M., Flamm, D. L., Eds. *Plasma Etching: An Introduction*; Academic Press: New York, 1989.

(27) Gebelein, C. G., Dunn, R. L., Eds. *Progress in Biomedical Polymers*; Plenum Press: New York, 1988.

(28) Griesser, H. J.; Chatelier, R. C. *J. Appl. Polym. Sci., Appl. Polym. Sym.* **1990**, *46*, 361.

(29) Griesser, H. J.; Youxian, D.; Hughes, A. E.; Gengenbach, T. R.; Mau, A. W. *Langmuir* **1991**, *7*, 2484.

(30) Hughes, A. E.; Sexton, B. A. *J. Electron Spectrosc. Relat. Phenom.* **1988**, *46*, 31.

(31) Scofield, J. H. *J. Electron Spectrosc. Relat. Phenom.* **1976**, *8*, 129.

(32) Griesser, H. J.; Gengenbach, T. R.; Dai, L.; Li, S.; Chatelier, R. C. *J. Adhesion Sci. Technol.*, in press.

(33) Yasuda, H. K., Ed. *J. Appl. Polym. Sci., Appl. Polym. Symp.* **1988**, *42*; **1990**, *46*. Gengenbach, T. R.; Chatelier, R. C.; Vasic, Z. R.; Griesser, H. J. *ACS Polym. Prep.* **1993**, *34*, 687.

(34) Dai, L.; Zientek, P.; St Johns, H.; Pasic, P.; Chatelier, R.; Griesser, H. J. In *Surface Modification of Polymeric Biomaterials*, Ratner, B. D., Castner, D., Eds.; Plenum Press: New York, 1996. Chatelier, R. C.; Dai, L.; Griesser, H. J.; Li, S.; Zientek, P.; Lohmann, D.; Chabrecek, P. *PCT Int. Appl. WO 94 06, 485* (CA121:18126).

(35) Vargo, T. G.; Thompson, P. M.; Gerenser, L. J.; Valentini, R. F.; Aebischer, P.; Hook, D. J.; Gardella, J. A., Jr. *Langmuir* **1992**, *8*, 130.

(36) Wilbur, J. L.; Biebuyck, H. A.; MacDonald, J. C.; Whitesides, G. M. *Langmuir* **1995**, *11*, 825. Takami, T.; Delamarche, E.; Michel, B.; Gerber, Ch.; Wolf, H.; Ringsdorf, H. *Langmuir* **1995**, *11*, 3876. Krausch, G.; Hipp, M.; Boltau, M.; Marti, O.; Mlynek, J. *Macromolecules* **1995**, *28*, 260.